Charge-state changing processes for Ne ions passing through thin carbon foils

A. Blažević, H. G. Bohlen, and W. von Oertzen*
Hahn-Meitner-Institut GmbH, Glienicker Straße 100, D-14109 Berlin, Germany
(Received 25 August 1999; published 15 February 2000)

We report on a method to measure charge-changing cross sections for ions passing through matter *in nonequilibrium conditions*. The charge states of an initial distribution are separated by applying a high voltage before they penetrate thin carbon foils; the charge states after those foils are identified using a high resolution magnetic spectrometer. Thus the full matrix of cross sections $\sigma(q_i,q_f)$ and energy losses $\Delta E(q_i,q_f)$ is obtained. The data are compared to calculated charge-state distributions based on microscopic cross sections for charge-changing processes in individual interaction steps and with a Monte Carlo simulation.

PACS number(s): 34.50.Bw, 79.20.Rf

I. INTRODUCTION

The proper understanding and calculation of the processes occuring when ions pass through matter have been the subject of intensive studies since the early work of Bethe [1] and Bohr [2]. In their investigations, the energy transferred in an atomic collision, and the specific energy loss for ion energies where the electronic energy loss dominates, were calculated by assuming a certain charge state of the ion. In general, an effective charge state q_{eff} has been introduced in order to describe the energy loss of ions in matter. The effective charge is a semiempirical quantity, which takes into account that an ensemble of ions develops a charge-state distribution during the passage through matter. It represents a weighted average over the various charge-dependent energy losses. In practice, q_{eff}^2 is used as a scale factor for the well known stopping power of protons at the same energy [4]. But it becomes a useful quantity only after several charge-changing collisions—at the charge equilibrium conditions. Various refinements of the well known Bethe-Bloch formula [3] for the specific energy loss dE/dx have been made over recent decades [4,5], usually by introducing correction terms, as, e.g., by Lindhard [6]. Essential ingredients in these approaches are the individual charge-changing collisions contributing to the final energy loss. The semiempirical approach for the specific energy loss of Ziegler *et al.* [4] gives a good description in the case of equilibrium charge states; however, it has its limits, e.g., for rather thin layers, where charge-changing collisions are not in equilibrium.

Another important aspect, which was apparent in the early work, is the strong variation of the electron-capture and electron-ionization probabilities for given electronic configurations in atoms as a function of the relative velocities. At energies higher than 1–2 MeV/u the ions are ionized in the higher shells and change their charge state rather quickly. Under these conditions equilibrium is reached for material layers up to $50\,\mu g/cm^2$ thickness.

The analysis of thin (10–100 nm) layer samples with ERDA (elastic recoil detection analysis) using a high resolution magnetic spectrometer has reached depth resolution limits of about 1 nm [7,8]. In these thin layers the incident ions usually have not yet reached the equilibrium charge-state distribution with a mean charge state q_{eq}, and hence suffer a smaller or higher energy loss, depending on whether the initial charge state is lower or higher than q_{eq}. For these applications it is of importance to have a detailed knowledge of the charge-changing processes in the first layers of the material studied. These are also of general interest for understanding of the passage of ions through matter. In the present work we report on a method to measure charge-changing processes and energy losses of ions in dependence on the initial and final charge states. These quantities are measured for various thicknesses of target foils, which will define various situations, nonequilibrium and the transition to equilibrium conditions. The results will serve to model microscopic theories in order to calculate the specific energy loss dE/dx of ions in very thin layers.

II. EXPERIMENTAL METHOD

In our measurements we use the high resolution magnetic spectrometer Q3D [9], which we have been using for the thin layer ERDA method at the Ion Beam Laboratory (ISL) at the Hahn-Meitner-Institut. The principle of the method presented in the present work is based on the production of a *charge-state distribution* of the incoming ions by a first, thin scattering foil and a *separation of the incoming charge states* q_i by applying a potential difference U between this foil and a second target foil as shown in Fig. 1. The transmission foil is used to study the processes of interest; the ions penetrating the foil lose energy and change their charge state with high probability. Energy analysis of the transmitted ions is obtained by a position-sensitive detector in the focal plane of the spectrometer, which selects one outgoing charge state q_f.

With this setup an intrinsic energy resolution of $\Delta E/E = 4\times10^{-4}$ was obtained. For this particular q_f, we observe several peaks in the focal plane spectrum, which are separated by the energy difference $\Delta E_U = \Delta q \times U$, corresponding to different initial charge states q_i, as shown in Figs. 1, 3, and 4 below. The intensities of the relevant lines, with varying q_i and fixed q_f, give the charge-changing cross sections; the whole matrix of $\sigma(q_i,q_f)$ is obtained by selecting the corresponding magnetic fields for the different q_f values. In addition to the charge-state distribution, the energy loss

*Also Fachbereich Physik, Freie Universität Berlin.

 ©2000 The American Physical Society

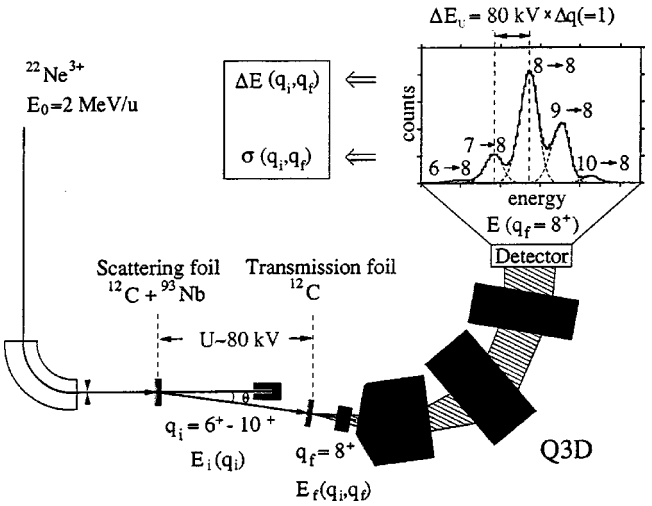

FIG. 1. The principle of the method to investigate charge-changing processes and energy loss as a function of the incoming (q_i) and outgoing (q_f) charge states of the projectile. A potential difference U is applied, which allows energetic separation of ions with different initial charge states q_i in front of and the same final charge state q_f behind the transmission foil.

$\Delta E(q_i,q_f)$ can be determined for the same parameter space, q_i and q_f. In the setup we used a thin layer of Nb (8 μg/cm^2) evaporated on a carbon backing (6 μg/cm^2) as scattering foil. This foil produces a charge-state distribution from the incident beam from the accelerator, which usually has a charge state far from equilibrium. It has to be a very thin and homogeneous foil so as to preserve the good energy resolution of the primary beam. The scattering angle is set in such a way that the count rate in the focal plane of the spectrometer is kept below a few kHz. By varying the thickness d of the transmission foil, the measurement allows the determination of two important quantities: the charge-changing cross section for each pair of q_i and q_f, $\sigma(q_i,q_f)$, and the energy loss $\Delta E(q_i,q_f,d)$ with the same selection of charge states q_i and q_f, as a function of foil thickness d.

III. THE EXPERIMENT: Ne IONS IN C FOILS

The present study was performed with a ^{22}Ne beam at an energy of 2 MeV/u, accelerated in a charge state of $q=+3$ in the cyclotron at ISL. At this energy the equilibrium charge state in the carbon medium is approximately given by $\bar{q} \approx 8.5$. The beam was scattered on a 8-μg/cm^2-thick Nb layer evaporated on a self-supporting C foil of 6 μg/cm^2 thickness. The measured charge-state distribution after this scattering foil is plotted in Fig. 2. It serves as the initial charge-state distribution for the transmission foil. The distance between the two foils was about 30 cm, long enough for all ions that left the scattering foil in an excited state to decay before they reached the transmission foil.

In Fig. 3 and Fig. 4 we show two examples of measured spectra for final charge states $q_f=+6$ and $q_f=+10$. The spectra are normalized to the same integrated current as the incident beam (normalization factor N_0). For two given q_f values (+6 and +10) the yields for individual q_i charge

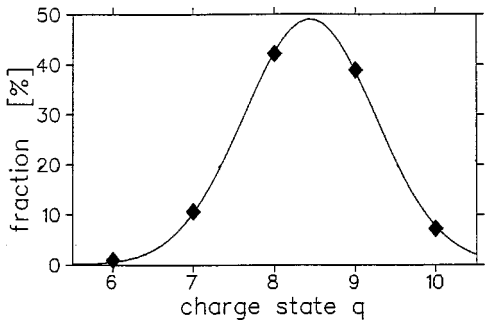

FIG. 2. Charge-state distribution of ^{22}Ne at 2 MeV/u after the scattering foil.

states are shown for foils varying in thickness between 0 and 18 μg/cm^2. The individual peaks for each charge state q_i are well separated with an applied potential difference of $U=80$ kV. The upper diagram shows the single line without the transmission foil. The subsequent graphs show the spectra in the focal plane of the magnetic spectrometer Q3D with increasing energy loss due to the increasing foil thickness d, as indicated. Five lines can be identified, from $q_i=+6$ on the left side up to $q_i=+10$ on the right side. We observe a broadening of the individual peaks with increasing target thickness due to straggling effects and a shift due to the energy loss $\Delta E(q_i,q_f,d)$. By unfolding the observed peaks we are able to extract the peak position (for the energy loss)

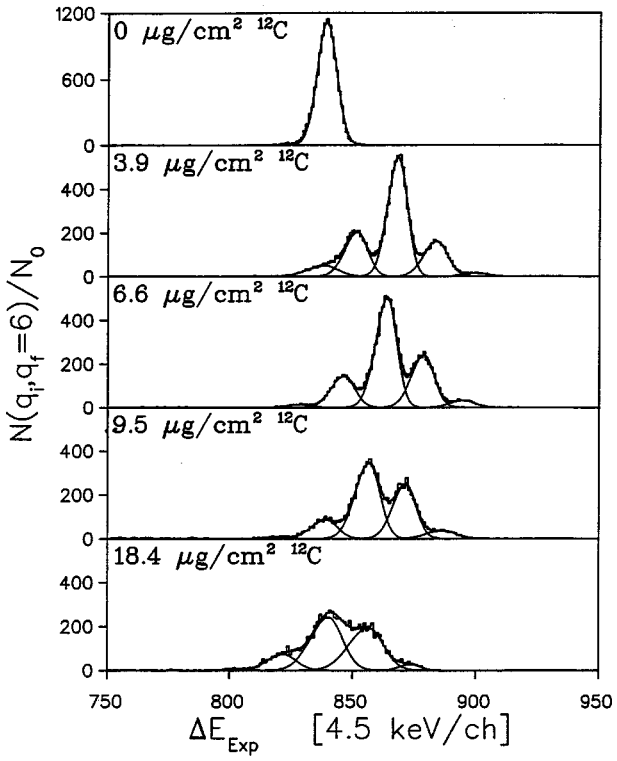

FIG. 3. Energy spectra of ^{22}Ne ions with an energy of 2 MeV/u and final charge state $q_f=+6$, normalized to the same integrated current as the incident beam, after passage through a ^{12}C transmission foil with varying thickness as indicated. The peaks for different q_i are shifted due to the potential difference U as explained in Fig. 1.

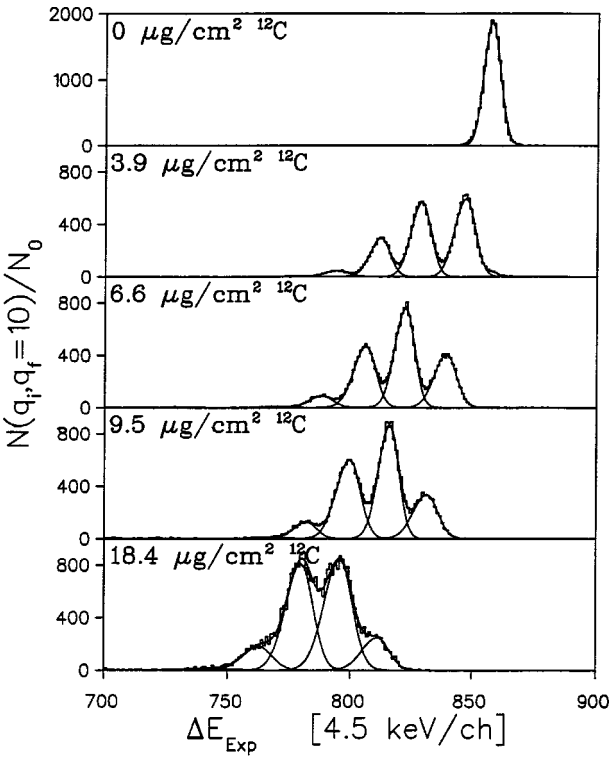

FIG. 4. The same as Fig. 3, but for $q_f=+10$.

and its integral (for the charge distribution) for each foil thickness and for each q_i. The information obtained from this procedure is the energy loss as well as the charge-state changing cross section as a function of target thickness and initial charge state, which allows us to study the evolution toward equilibrium for each q_i. The result is compiled in Fig. 5 for the charge states $q_i=+6$, $+7$, $+8$, $+9$, and $+10$, where the fractions (percentages) of each charge state q_f are shown as a function of the target thickness. The plotted error bars represent the statistical errors. The evolution of the charge-state distribution with increasing foil thickness can be clearly seen in the spectra. The equilibrium distribution at $d=50$ μg/cm^2, which is known from other work [10], has also been verified in a separate measurement.

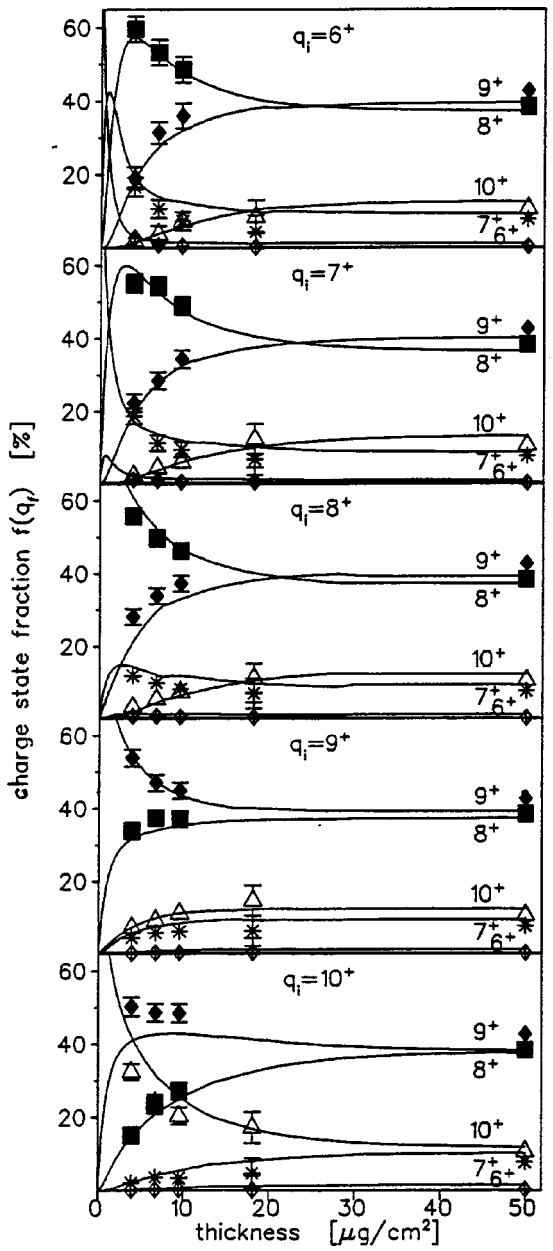

FIG. 5. Charge-state distributions for ^{22}Ne at 2 MeV/u for different initial charge states q_i ($+6$ to $+10$). The symbols show the measured values, the lines represent results for the charge-state fractions from the solution of the rate equations with the cross sections given in Table I.

IV. ANALYSIS OF THE CHARGE DISTRIBUTIONS

For the interpretation of these results, model calculations can be done in two ways: (1) by solving the coupled-channel rate equations for the individual charge-state probabilities [11], or, (2) by a Monte Carlo calculation, following the history of each ion on its way through the foil with the complete set of cross sections for different electronic configurations at each interaction step [8]. In this study both approaches have been pursued [8]. First we discuss briefly the results of the model of Rozet *et al.* [11], which are actually shown as full lines in Fig. 5.

A. Description of the charge-state distributions by solving the rate equations

For calculation of the charge-state distribution, where rates of charge-changing processes enter, the cross sections for all interaction processes and for each possible electronic configuration of the penetrating ion must be entered. These cross sections are electron capture σ_c (radiative and radiationless), ionization from a shell, σ_{ion}, excitation from one shell with quantum number n_i to a higher shell n_f, σ_{ex} (for shells with $n_f \leqslant 3$, for excitation to $n_f \geqslant 4$, σ_{ex} is added to σ_{ion} by estimating σ_{ex} for $n_f=4$ and using a $1/n^3$ scaling law for higher shells), and Auger and radiative decay. We used the code ETACHA [11] to calculate these cross sections for hydrogenlike configurations and then to scale them for the proper ionic charge, taking into account the screening effects of the residual electrons [11,12]. The data are very

TABLE I. Calculated cross sections (10^{-20} cm^2) for the atomic processes of Ne projectiles in their respective charge states in the ground state or with one electron in a higher shell (marked with *) passing through carbon.

σ	+6	+7	+8	+9	+10
$\sigma_c(1s)$				115	221
$\sigma_c(2s)$		46.7	106	135	160
$\sigma_c(2p)$	152	174	197	251	298
$\sigma_c(3s)$	11.0	19.1	30.5	48.8	72.0
$\sigma_c(3p)$	18.5	32.1	51.4	81.9	121
$\sigma_c(3d)$	7.3	12.8	20.4	32.5	48.0
$\sigma_{ion}(1s)$	143	135	126	50.1	
$\sigma_{ion}(2s)$	2370	1060	907*	757*	
$\sigma_{ion}(2p)$	1370*	1200*	1000*	838*	
$\sigma_{ion}(3s)$	3150*	2890*	2620*	2330*	
$\sigma_{ion}(3p)$	3260*	3000*	2720*	2430*	
$\sigma_{ion}(3d)$	3300*	2980*	2700*	2450*	
$\sigma_{ex}(1s\rightarrow 2s)$		6.9	13.5	6.1	
$\sigma_{ex}(1s\rightarrow 2p)$	75.5	72.0	68.4	28.3	
$\sigma_{ex}(1s\rightarrow 3s)$	2.9	2.8	2.8	1.3	
$\sigma_{ex}(1s\rightarrow 3p)$	14.4	13.7	12.9	5.3	
$\sigma_{ex}(1s\rightarrow 3d)$	1.4	1.3	1.3	0.5	
$\sigma_{ex}(2s\rightarrow 2p)$	2070	1030	1030*	1030*	
$\sigma_{ex}(2s\rightarrow 3s)$	151	72	66*	56*	
$\sigma_{ex}(2s\rightarrow 3p)$	206	99	93*	81*	
$\sigma_{ex}(2s\rightarrow 3d)$	598	279	253*	210*	
$\sigma_{ex}(2p\rightarrow 3s)$	40*	35*	30*	26*	
$\sigma_{ex}(2p\rightarrow 3p)$	92*	85*	77*	81*	
$\sigma_{ex}(2p\rightarrow 3d)$	362*	343*	317*	210*	

sensitive to the values of the cross sections, in particular in those cases where a fast change of the charge yield is observed in the thinnest layer of 3.9 μg/cm^2. In a first attempt we got a quite good description of the data for low q_i (+6 and +7), indicating that the ionization and excitation cross sections were correct, but there were obvious discrepancies for $q_i=+10$, where only electron capture contributes in the first steps. We concluded that the calculated capture cross sections have to be improved. Rozet *et al.* [11] use the eikonal approximation for relativistic projectiles suggested by Eichler [13] for the capture calculations. The predictions of this approximation agree well at high energies with those of the *continuum distorted wave approximation* (CDWA), but give too small cross sections for an intermediate energy of 2 MeV/u. So we have used the values from the CDWA [14] and got satisfactory agreement with the data in Fig. 5. We would like to point out that there is no fitting parameter in this description. The cross sections we used to calculate the curves shown in Fig. 5 are compiled in Table I. From these cross sections and from Fig. 5 we can identify the processes that contribute most to a change of the charge states. (1) σ_c, the capture cross sections for $q_i=+9$ and +10, are large into electronic states that are velocity matched for 2 MeV/u (mostly transitions into $1s$ and $2p$). (2) σ_{ion}, ionization cross sections from the higher shells (in particular from $2p,3s$, and higher states), are large. (3) σ_{ex}, the dipole transitions ($1s\rightarrow 2p, 2s\rightarrow 2p$), are comparable to σ_{ion} and are mostly followed by the ionization of the excited electron.

B. Monte Carlo simulation of the charge-state distributions

The second way to describe the charge-state distributions is a Monte Carlo simulation (MCS). We used the same routines as in ETACHA to calculate the cross sections for the processes listed before for all possible electronic configurations, distributed over the K, L, and M shells. Starting from a given configuration, namely, the ground state configuration for the incident charge states, we calculated the cross sections and the rates mentioned above. With the random generator RANLUX [15] we determined for each step of the passage through the foil with a step size of 0.1 μg/cm^2, whether a charge exchange occurred or not, and, if yes, for which process (capture, ionization, excitation, or decay). In the case that a transition had occurred, a new set of cross sections according to the new electronic configuration was calculated for the next step. The number of steps varied from 39 for the thinnest foil to 185 for the thickest one. Smaller step sizes have been tested, but have not led to different results. The simulated charge-state distributions obtained in this way agree well with the data as well as with the distributions from the rate equations. However, in this description of the processes we get additional information about the passage of the ion through the foil. Figure 6 shows as an example the details of the MCS for a Ne ion with an initial charge state $q_i=+10$ passing through a carbon foil of 3.8 μg/cm^2 thickness. Starting with a given number of particles on the left side, an upward branch shows the number of ions that have captured an electron. A horizontal branch points to the number of projectiles passing the foil without further charge-changing reaction, and a branch downward indicates how many ions have lost an electron. At the very right side, the final charge states after 39 interaction steps are plotted in angular brackets. We can see that out of 1 million incident particles, 183 302 traverse the foil in a frozen charge state, that is, about 43% of all the ions with the final charge state $q_f=+10$. Of the 816 698 particles that have captured an electron, 327 036 lost it again, but only half of them crossed the foil without any further charge exchange. The other half captured another electron. 32 957 of these ions were ionized once more and left the foil again with $q_f=+10$ (7.0%). 29 380 particles captured two electrons before they lost them again (7.8%). With this detailed picture a detailed assessment of the energy loss as a function of charge states in thin foils also becomes possible.

C. Charge-state-dependent energy loss

Detailed knowledge of the charge-changing processes during the transition of ions through matter is an important aspect of the energy loss of the ions. In the following discussion we consider as an example the energy loss for the transition $q_i=+10$ and $q_f=+10$. As long as the ^{22}Ne ions are in a charge state lower than +10, they have a smaller stopping power, and so they will modify the finite value of the energy loss $\Delta E(q_i=+10, q_f=+10)$ of ions without charge exchange (frozen charge state). Our measured results for the

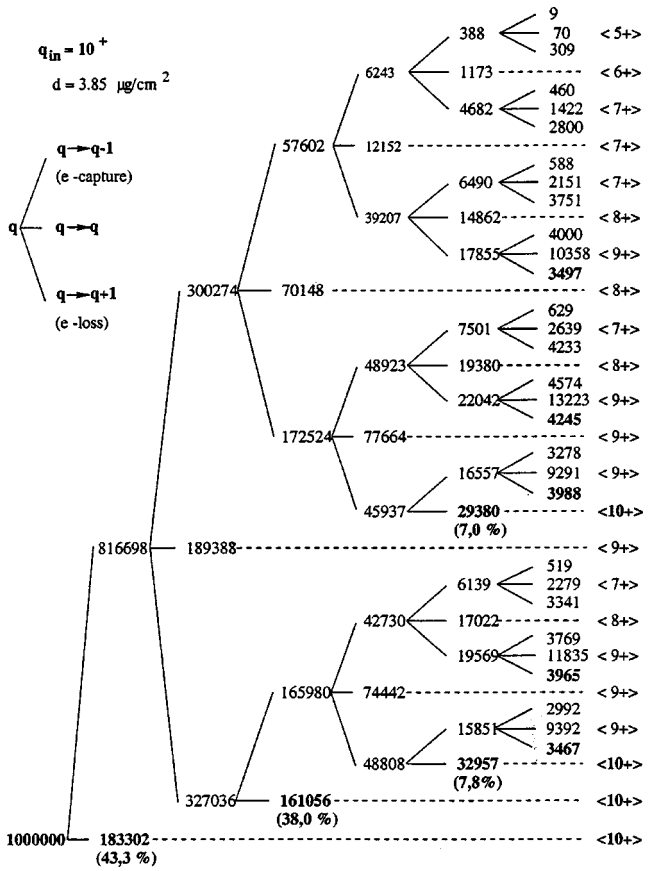

FIG. 6. Monte Carlo simulation of the passage of a ^{22}Ne ion at 2 MeV/u and an initial charge state $q_i=+10$ through a 3.8 μg/cm^2 thick carbon foil. The branching for each interaction step is explained in the upper left. The values in parentheses indicate the percentage of ions with respect to the total number of ions in the final charge state $q_f=+10$ (bold numbers). The final charge states at the exit from the foil, $\langle q_f \rangle$, are indicated on the right side.

charge dependence of the energy loss $\Delta E(q_i,q_f,d)$ are shown in Fig. 7, where from our complete matrix only the energy losses for $q_i=q_f$ are shown. In order to estimate the influence on the ΔE values of those ions that had some charge-state fluctuations before they left the foil with q_f, we have to take a look at the cross sections of Table I. For the charge state $+10$ we see that most electrons are captured into the $2p$ shell (32%), followed by the $1s$ shell (24%) and the $2s$ shell (17%). The electrons in the $2p$ shell are ionized with high probability [$\sigma_{ion}(2p,+9)=838\times10^{-20}$ cm^2] and those in the $2s$ shell also [$\sigma_{ion}(2s,+9)=757\times10^{-20}$ cm^2]. For the $2s$ shell there is another very high cross section leading to the depopulation of the $2s$ configuration: the excitation to the $2p$ shell [$\sigma_{ex}(2s\rightarrow2p,+9)=1030\times10^{-20}$ cm^2]. Those large cross sections especially lead to small mean free path values λ[$\lambda(2s)=0.9$ μg/cm^2, $\lambda(2p)=1.7$ μg/cm^2], whereas the ground state configuration is much more stable [$\lambda(1s)=23.1$ μg/cm^2]. Consequently, the particles that left the foil with $q_f=+10$ but which were temporarily in the charge state $+9$, where the electron was captured into a higher shell ($2s$ or $2p$), will not influence the $\Delta E(q_i=+10,q_f=+10)$ value too much.

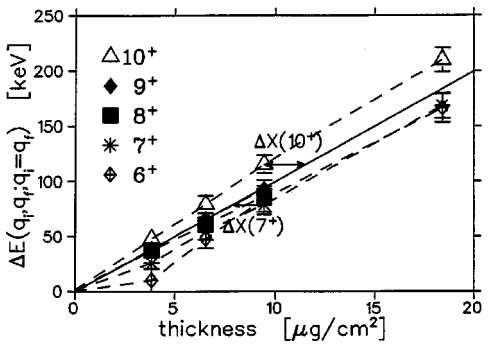

FIG. 7. Measured energy loss of 2 MeV/u ^{22}Ne for different charge states $q_i=q_f$ as a function of the thickness of the carbon foils. The solid line represents the energy loss calculated in the conventional way using the values for the charge-state equilibrium; the dashed lines are drawn to guide the eye. For illustration we have marked by arrows the energy loss error and thus the foil thickness difference ΔX between the ΔE value represented by the full line and our measurement for $q_i=+7$ and $q_i=+10$, respectively.

However, those ions (24%) that captured an electron in the $1s$ shell will change the measured value the most.

In Table II we give a compilation of quantities of this type for understanding the energy loss $\Delta E(q_i=q_f)$. We have listed the percentage values as in Fig. 6 for all measured q_i. A ''c'' symbolizes an electron capture; ''l'' is for the ionization process. According to the argument given above we can conclude that the measured values of ΔE for the thinnest foil in Fig. 7 and for the charge states $q_i=+8$ to $+10$ correspond mainly to the frozen charge states, whereas the values for $q_i=+7$ and $+6$ were generated mostly by the charge state $+8$. Hence, the fractional stopping powers cannot be determined directly from the slopes of the curves in Fig. 7, because the contributions to ΔE from the charge-state fluctuations increase with the foil thickness, so that the ΔE values for the thicker foils differ from the frozen charge-state energy losses.

V. CONCLUSIONS AND OUTLOOK

With the method presented here it is possible to investigate efficiently the charge-state distributions and energy

TABLE II. Percentage of ^{22}Ne ions with $q_i=q_f$ that have suffered charge-changing fluctuations in a carbon foil of 3.8 μg/cm^2 thickness. c, electron capture; l, electron loss.

Process	+10	+9	+8	+7	+6
no	43.3	46.5	52.9	13.5	2.9
c-l	38.0	34.4	29.3	12.7	3.5
l-c		2.8	5.5	40.2	30.5
c-c-l-l	7.0	5.1	3.1	1.5	0.4
c-l-c-l	7.8	6.2	4.4	3.4	1.1
c-l-l-c		0.8	1.1	6.0	4.5
l-c-c-l		0.5	0.8	5.3	4.6
l-c-l-c		0.5	0.8	8.0	12.1
l-l-c-c			0.1	2.2	21.0
6 and more	3.9	3.2	2.0	7.2	19.5

losses of ions in thin foils as a function of initial and final charge state. These quantities were measured for Ne ions at an energy of 2 MeV/u penetrating carbon foils of varying thicknesses (3.8–50 $\mu g/cm^2$). The measured charge-state evolutions for different initial charge states ($+6$ to $+10$) can be described by solving the rate equations; the needed cross sections were calculated. We got satisfying agreement with the measured data without any fitting parameter. With these cross sections a Monte Carlo simulation code was written to investigate the charge-changing history of the ions during their passage through the foil. In connection with the measured energy losses for ions that enter and leave the foil with the same charge state, $q_i = q_f$, we were able to estimate the contributions of those ions that suffered several charge-state fluctuations to the energy loss of those ions that passed the foil in a frozen charge state. This investigation led to the conclusion that the stopping power for frozen charge states could not be extracted from the slopes of the measured energy loss data. This point will be the subject of a future study.

An interesting quantity that will be analyzed in more detail in further work is the energy loss and its dependence on the initial and final charge states. Such measurements have been reported previously also using magnetic spectrometers [7,16,17] by selecting initial charge states of ions from the accelerator. Those measurements have estimated only the energy losses for $q_i = q_f$. Our method allows us to measure the energy losses for all combinations of incident and final charge states. These data can now be put into a quantitative relation to the elementary processes by using the full matrix of $\sigma(q_i, q_f)$ and $\Delta E(q_i, q_f)$. The aim is to eliminate the contributions to the measured energy losses of those ions that have undergone charge-changing fluctuations, and to extract frozen-charge-state stopping powers. Finally, it should be possible to estimate the energy loss of ions with high precision, even in very thin layers, where charge-state equilibrium is not yet reached. This will give a reliable basis for applications of ion beams using ERDA for the analysis of very thin films in the nanometer range as discussed by Dollinger *et al.* [7,18]. In addition to this, the technique described here will give experimental access to detailed data on the processes governing the passage of ions in matter.

ACKNOWLEDGMENTS

We thank Severin Thummerer and Christian Schulz for their help during the experiment, G. Schiwietz for helpful discussions, and J. P. Rozet for the support of our work as well as for making the code for coupled rates available to us.

[1] H. A. Bethe, Z. Phys. **76**, 293 (1932).
[2] N. Bohr, Mat. Fys. Medd. K. Dan. Vidensk. Selsk. **18**, 8 (1948).
[3] F. Bloch, Ann. Phys. (Leipzig) **16**, 285 (1933).
[4] J. F. Ziegler, J. P. Biersack, and U. Littmark, *The Stopping and Range of Ions in Solids* (Pergamon Press, New York, 1985).
[5] J. Lindhard and M. Scharff, Phys. Rev. **124**, 128 (1961).
[6] J. Lindhard, Nucl. Instrum. Methods **132**, 1 (1976).
[7] G. Dollinger *et al.*, Nucl. Instrum. Methods Phys. Res. B **136–138**, 574 (1998).
[8] A. Blažević, Ph.D. thesis, Freie Universität Berlin, 1998.
[9] H. G. Bohlen, *Symposium on Detectors in Heavy Ion Reactions*, Lecture Notes in Physics, Vol. 178 (Springer, Heidelberg, 1983), p. 105.
[10] H. Shima, T. Ishihara, and T. Mikumo, Nucl. Instrum. Methods Phys. Res. **200**, 605 (1982).
[11] J. P. Rozet, C. Stéphan, and D. Vernhet, Nucl. Instrum. Methods Phys. Res. B **107**, 67 (1996).
[12] R. Anholt, Phys. Rev. A **31**, 3579 (1985).
[13] J. Eichler, Phys. Rev. A **23**, 498 (1981).
[14] Dz. Belkic, R. Gayet, and A. Salin, Comput. Phys. Commun. **23**, 153 (1981).
[15] F. James, Comput. Phys. Commun. **79**, 111 (1994).
[16] H. Ogawa *et al.*, Nucl. Instrum. Methods Phys. Res. B **82**, 80 (1993).
[17] J. F. Pendler and H. J. Hay, Nucl. Instrum. Methods Phys. Res. B **4**, 72 (1994).
[18] G. Dollinger *et al.*, Nucl. Instrum. Methods Phys. Res. B **136-138**, 603 (1998).